Transactions of the ASME Journal of Dynamic Systems, Measurement, and Control, Vol. 124, No. 4, pp. 704-709, 2002.

Two-Degree-of-Freedom Optimal Preview Tracking Control –A Mechatronic Design Example–

Jin-Hua She[†,*] Xin Xin[‡] and Yasuhiro Ohyama[†]

[†] Department of Mechatronics, School of Engineering
Tokyo University of Technology
1404-1 Katakura, Hachioji, Tokyo, 192-0982 Japan
Phone & Fax: +81(426)37-2487
E-mail: {she, ohyama}@cc.teu.ac.jp

[‡] Department of Communication Engineering
Faculty of Computer Science and System Engineering
Okayama Prefectural University
111 Kuboki, Soja, Okayama, 719-1197 Japan
Phone & Fax: +81(866)94-2131
E-mail: xxin@c.oka-pu.ac.jp

Abstract. A design method for digital tracking control is described and applied to control an arm robot with structured uncertainties. A two-degree-of-freedom control system configuration provides the desired feedback and input-output performances independently. Regarding controller design, first, sampled-data $\mathcal{H}_\infty$ control and linear matrix inequality approaches are used to design a reduced-order output feedback controller. Then, the feedforward controller is parameterized based on the feedback controller, with the free parameter being chosen based on a preview strategy.

1 Introduction

A two-degree-of-freedom (TDF) control system configuration (e.g., [1,2]) provides tracking control with good closed-loop and tracking performances independently.

Many mechatronic systems are modeled as a linear continous time-invariant system (the nominal plant) with continous-time uncertainties. The use of a microcomputer device as a controller makes the sampled-data control system periodic, even if both the plant and controller are time-invariant. This makes it difficult to synthesize the

* Corresponding author

sampled-data system. Note that sampled-data $\mathcal{H}_\infty$ control, which handles the continuous uncertainties of a plant directly, has provoked a great deal of interest (e.g., [3,4]), and that the performance of a control system can be improved by constructively using information about future inputs [5-7].

This paper integrates TDF control, sampled-data $\mathcal{H}_\infty$ control and preview control into a new design method for a digital tracking control system for a continuous plant with structured uncertainties. The design of the feedback controller is formulated as a sampled-data $\mathcal{H}_\infty$ control problem. Since the order of an $\mathcal{H}_\infty$ controller is usually very high, the results in [8] are used to reduce it. The feedforward controller is parameterized based on the feedback controller, and an optimal preview tracking feedforward controller is constructed. This design method was applied to the positioning control of an arm robot [9] to demonstrate the validity of the method.

2 Problem Formulation

Consider the TDF tracking control system configuration in Fig. 1, which is a slight extension of one proposed by Hara and Sugie [2]. $P(s)$ is a plant with structured uncertainties:

$$\begin{cases} \dot{x}_P(t) = (A_P + \Phi\Gamma(t)\Psi_A)x_P(t) + (B_P + \Phi\Gamma(t)\Psi_B)u_P(t), \\ y(t) = C_P x_P(t), \end{cases} \tag{1}$$

where $x_P(t) \in \mathbf{R}^{n_P}$, $y(t) \in \mathbf{R}$ and $u_P(t) \in \mathbf{R}$ are the state, output and control input of the plant, respectively. Note that $A_P, B_P, C_P, \Phi, \Psi_A$ and Ψ_B are constant real matrices, and $\Gamma(t)$ is an unknown bounded matrix ($\Gamma^T(t)\Gamma(t) \leq I$) that represents the time-varying parameter uncertainties. Without loss of generality, $C_P = [c_{P1} \quad 0]$, $c_{P1} \neq 0$ ($c_{P1} \in \mathbf{R}$) is assumed. The nominal plant, $P_0(s)$, is given by the triplet (A_P, B_P, C_P).

Let the reference input be ($\lambda := z^{-1}$)

$$\begin{cases} r(\lambda) = \dfrac{\bar{r}(\lambda)}{\phi_R(\lambda)}, \quad \bar{r}(\lambda) = \displaystyle\sum_{i=0}^{L-1} r_i \lambda^i; \\ \phi_R(\lambda) = 1 + \phi_1\lambda + \ldots + \phi_L\lambda^L \end{cases} \tag{2}$$

with all the roots of $\phi_R(\lambda) = 0$ being in the closed unit circle, where $1/\phi_R(\lambda)$ is the generator of the reference input and $\bar{r}(\lambda)$ is the initial function. Then, the internal model of the reference input, $M_R(\lambda)$, is

$$\begin{cases} x_R[i+1] = A_R x_R[i] + B_R e_R[i], \\ A_R = \begin{bmatrix} 0 & 1 & & \mathbf{0} \\ \vdots & & \ddots & \\ 0 & \mathbf{0} & & 1 \\ -\phi_L & -\phi_{L-1} & \ldots & -\phi_1 \end{bmatrix} \in \mathbf{R}^{L\times L}, \\ B_R = [0 \quad \ldots \quad 0 \quad 1]^T \in \mathbf{R}^{L\times 1}. \end{cases} \tag{3}$$

This paper considers the following design problems.

(a) Design a reduced-order feedback controller $K_2(\lambda)$ ($K_2(\lambda) = [\,K_{2P}(\lambda) \quad K_{2R}(\lambda)\,]$, $u_P[i] = K_2(\lambda)\begin{bmatrix} y[i] \\ x_R[i] \end{bmatrix}$) with an order less than n_P, that robustly stabilizes the control system in Fig. 1.

(b) Design a feedforward controller $K_1(\lambda)$ that yields the desired nominal input-output tracking performance.

3 Design of Feedback Controller

Redrawing Fig. 1 with $r[i] = 0$ gives Fig. 2. The new signals $v(t)$ and $w(t)$ are defined to be the input and output of the uncertainty $\Gamma(t)$, respectively; and $v_u(t)$, $v_P(t)$ and $v_R[i]$, are the control input, and the states of the plant and internal model weighted by positive semi-definite matrices $Q_u^{1/2}$, $Q_P^{1/2}$ and $Q_R^{1/2}$, respectively.

Applying the small gain theorem of a sampled-data system [10] to the control system in Fig. 1 yields the following condition for robust stability:

$$\|\mathcal{G}_{\mathcal{P}}\|_\infty := \sup_{w(t)\in\mathbf{L}_2} \frac{\|v(t)\|_2}{\|w(t)\|_2} < 1. \tag{4}$$

To guarantee robust stability and obtain the desired closed-loop performance, we extend the controlled output to be $v_a := \begin{bmatrix} v(t) & v_u(t) & v_P(t) & v_R[i] \end{bmatrix}^T$. Then, the design problem for the feedback controller can be formulated as:

Find a reduced-order feedback controller $K_2(\lambda)$ that internally stabilizes the generalized plant $\mathcal{P}_\mathcal{S}$:

$$\begin{bmatrix} v_a \\ \hdashline y[i] \\ x_R[i] \end{bmatrix} = \mathcal{P}_\mathcal{S} \begin{bmatrix} w(t) \\ \hdashline u_P[i] \end{bmatrix} \tag{5}$$

and satisfies $\|\mathcal{G}_{\mathcal{P}_\mathcal{S}}\|_\infty < 1$, where $\mathcal{G}_{\mathcal{P}_\mathcal{S}} = \mathcal{P}_\mathcal{S} * K_2(\lambda) = \mathcal{P}_{\mathcal{S}11} + \mathcal{P}_{\mathcal{S}12}K_2(\lambda)[I - \mathcal{P}_{\mathcal{S}22}K_2(\lambda)]^{-1}\mathcal{P}_{\mathcal{S}21}$ is the linear fraction transformation (LFT) of $\mathcal{P}_\mathcal{S}$ and $K_2(\lambda)$, and $\mathcal{P}_\mathcal{S}$ is given by

$$\mathcal{P}_\mathcal{S} = \begin{bmatrix} \mathcal{P}_{\mathcal{S}11} & \mathcal{P}_{\mathcal{S}12} \\ \mathcal{P}_{\mathcal{S}21} & \mathcal{P}_{\mathcal{S}22} \end{bmatrix} = \left[\begin{array}{cc|c:c} A_R & -B_R\mathcal{S}_\tau C_P & 0 & 0 \\ 0 & A_P & \Phi & B_P\mathcal{H}_\tau \\ \hline 0 & \Psi_A & 0 & \Psi_B\mathcal{H}_\tau \\ 0 & 0 & 0 & Q_u^{1/2}\mathcal{H}_\tau \\ 0 & Q_P^{1/2} & 0 & 0 \\ Q_R^{1/2} & 0 & 0 & 0 \\ \hdashline 0 & \mathcal{S}_\tau C_P & 0 & 0 \\ I_L & 0 & 0 & 0 \end{array}\right]. \tag{6}$$

Note that the generalized plant $\mathcal{P}_\mathcal{S}$ contains both continuous and discrete parts. We first convert the design problem for the feedback controller to an equivalent discrete-time $\mathcal{H}_\infty$ control problem by the following steps:

Step 1 Partition the generalized plant $\mathcal{P}_\mathcal{S}$ in Fig. 2 into two sub-systems: a continuous subsystem, $P_C(s) : \begin{bmatrix} w(t) \;\vdots\; u_P(t) \end{bmatrix}^T \rightarrow \begin{bmatrix} v(t) & v_u(t) & v_P(t) \;\vdots\; y(t) \end{bmatrix}^T$; and a discrete subsystem, $P_D(\lambda) : \begin{bmatrix} y[i] \;\vdots\; u_P[i] \end{bmatrix}^T \rightarrow \begin{bmatrix} u_P[i] & v_R[i] \;\vdots\; y[i] & x_R[i] \end{bmatrix}^T$.

Step 2 Lift the continuous sub-system $P_C(s)$ and obtain the equivalent finite-dimensional discrete-time time-invariant system $\check{P}_C(\lambda)$

Step 3 Combine $\check{P}_C(\lambda)$ with the discrete sub-system $P_D(\lambda)$ using an LFT to obtain the equivalent generalized plant $P_e(\lambda) = \check{P}_C(\lambda) * P_D(\lambda)$.

Now, the design problem becomes to find a reduced-order feedback controller $K_2(\lambda)$ that internally stabilizes the equivalent discrete-time generalized plant $P_e(\lambda)$ and satisfies $\|P_e(\lambda) * K_2(\lambda)\|_\infty < 1$. If the result of Gahinet and Apkarian [11] were directly used to find an $\mathcal{H}_\infty$ controller, the order of the feedback controller would generally be $n_L = L + n_P$. To design reduced-order feedback controllers, we apply the results in Xin *et al.* [8] and obtain the following.

THEOREM 1 *Suppose the discrete-time $\mathcal{H}_\infty$ control problem for the generalized plant $P_e(\lambda)$ is solvable, then a feedback controller, $K_2(\lambda)$, with an order less than or equal to $n_P - 1$ can be constructed.*

4 Design of Feedforward Controller

Let the coprime factorizations of the nominal plant $P_0(\lambda)$ and the local feedback controller $K_{2P}(\lambda)$ be $P_0(\lambda) = N_P(\lambda)/D_P(\lambda)$; $K_{2P}(\lambda) = N_{2K}(\lambda)/D_{2K}(\lambda)$; $N_P(\lambda), N_{2K}(\lambda), D_P(\lambda), D_{2K}(\lambda) \in \mathbf{R}[\lambda]$, where $\mathbf{R}[\lambda]$ is a ring of polynomials in λ. Then, the transfer function of $P_0(\lambda)$ with local feedback $K_{2P}(\lambda)$ is $G(\lambda) = P_0(\lambda)/[1 + K_{2P}(\lambda)P_0(\lambda)]$. Also, let its coprime factorization be

$$G(\lambda) = \frac{N_G(\lambda)}{D_G(\lambda)}, \quad N_G(\lambda), D_G(\lambda) \in \mathbf{R}[\lambda]. \tag{7}$$

From Fig. 1, it is clear that the transfer functions from $r[i]$ to $y[i]$ and from $r[i]$ to $u_P[i]$ are

$$G_{yr}(\lambda) = N_G(\lambda)K_1(\lambda); \tag{8}$$

$$G_{u_P r}(\lambda) = D_P(\lambda)D_{2K}(\lambda)K_1(\lambda), \tag{9}$$

respectively. The transfer function of the weighted Eq. (9) is

$$G_{u_W r}(\lambda) = W_u(\lambda)G_{u_P r}(\lambda) := \frac{D_u(\lambda)}{N_u(\lambda)}K_1(\lambda), \tag{10}$$

where $N_u(\lambda), D_u(\lambda) \in \mathbf{R}[\lambda]$ are assumed to be coprime, and $W_u(\lambda)$ is a selected stable weighting transfer function.

Equations (8) and (10) show that the desired nominal input-output performance can be achieved by choosing a suitable feedforward controller, $K_1(\lambda)$. In many designs, $K_1(\lambda)$ is chosen from $\mathbf{RH}_\infty$. However, in this paper, the assumption that information about future inputs can be used allows the class of $K_1(\lambda)$ to be expanded from $\mathbf{RH}_\infty$ to the stable improper class, $\mathbf{R}_*$ (a set of real-rational functions in λ which have no poles in the closed unit circle except for the origin). In this paper, $K_1(\lambda)$ is designed to satisfy the following conditions:

(1) Deadbeat condition: The tracking error $e(\lambda) = r(\lambda) - y(\lambda) = \sum_{i=-\infty}^{\infty} e_i\lambda^i$ is a finite polynomial in λ and z. i.e., $e(\lambda) \in \mathbf{R}[\lambda] \cup \mathbf{R}[z]$.

(2) Low-ripple condition: The transfer function (10) is a finite polynomial in λ and z. i.e., $G_{u_W r}(\lambda) \in \mathbf{R}[\lambda] \cup \mathbf{R}[z]$.

Decomposing $N_G(\lambda)$ and $D_u(\lambda)$ into

$$N_G(\lambda) = N_G^+(\lambda)N_G^-(\lambda); \quad D_u(\lambda) = D_u^+(\lambda)D_u^-(\lambda), \tag{11}$$

where $N_G^+(\lambda)$ and $D_u^+(\lambda)$ ($N_G^-(\lambda)$ and $D_u^-(\lambda)$) denote polynomials with roots in/on (outside) the closed unit circle. And let $M(\lambda) \in \mathbf{R}[\lambda]$ be the greatest common divisor of $N_G^-(\lambda)$ and $D_u^-(\lambda)$. Then, all the feedforward controllers that satisfy the low-ripple condition are

$$K_1(\lambda) = \frac{N_u(\lambda)}{M(\lambda)}\bar{K}_1(\lambda), \quad \bar{K}_1(\lambda) \in \mathbf{R}[\lambda] \cup \mathbf{R}[z]. \tag{12}$$

Substituting Eq. (12) into Eqs. (8) and (10) yields

$$\begin{cases} G_{yr}(\lambda) = N(\lambda)\bar{K}_1(\lambda); & N(\lambda) := \dfrac{N_G(\lambda)}{M(\lambda)}N_u(\lambda) \in \mathbf{R}[\lambda], \\ G_{u_W r}(\lambda) = D(\lambda)\bar{K}_1(\lambda); & D(\lambda) := \dfrac{D_u(\lambda)}{M(\lambda)} \in \mathbf{R}[\lambda]. \end{cases} \tag{13}$$

Thus, the problem of designing the feedforward controller becomes that of designing $\bar{K}_1(\lambda)$ such that the deadbeat condition is satisfied.

Without loss of generality, assume

$$\begin{cases} D(\lambda) = a_0 + a_1\lambda + \cdots + a_n\lambda^n; \quad a_0, a_n \neq 0, \\ N(\lambda) = \lambda^m b(\lambda), \\ b(\lambda) = b_0 + b_1\lambda + \cdots + b_l\lambda^l; \qquad b_0, b_l \neq 0. \end{cases} \tag{14}$$

From the interpolation theorem, the $\bar{K}_1(\lambda)$ in (13) that yields low-ripple deadbeat control with a minimum settling-time is given by

$$\bar{K}_1^*(\lambda) = \frac{1 - \phi_R(\lambda) f^*(\lambda)}{N(\lambda)} \in \mathbf{R}[\lambda], \tag{15}$$

where

$$f^*(\lambda) = f_0^* + f_1^*\lambda + \cdots + f_{m+l-1}^*\lambda^{m+l-1} \tag{16}$$

and the coefficients are determined by the following steps. (For simplicity, we assume that $b(\lambda) = 0$ has only simple roots, which are denoted by $\lambda_1, \lambda_2, \cdots, \lambda_l$.)

Step 1 $f_0^*, f_1^*, \cdots, f_{m-1}^*$ are determined by $\phi_R(\lambda)$ and the m-multiple original zero of $N(\lambda)$:

If $L > m-1$,

$$\begin{bmatrix} f_0^* \\ f_1^* \\ \vdots \\ f_{m-1}^* \end{bmatrix} = \begin{bmatrix} 1 & & & \mathbf{0} \\ \phi_1 & \ddots & & \\ \vdots & \ddots & \ddots & \\ \phi_{m-1} & \cdots & \phi_1 & 1 \end{bmatrix}^{-1} \begin{bmatrix} 1 \\ 0 \\ \vdots \\ 0 \end{bmatrix}; \tag{17}$$

and if $L \leq m-1$,

$$\begin{bmatrix} f_0^* \\ f_1^* \\ \vdots \\ f_L^* \\ \vdots \\ f_{m-1}^* \end{bmatrix} = \begin{bmatrix} 1 & & & & & \mathbf{0} \\ \phi_1 & \ddots & & & & \\ \vdots & \ddots & \ddots & & & \\ \phi_L & \ddots & \ddots & \ddots & & \\ & \ddots & \ddots & \ddots & \ddots & \\ \mathbf{0} & & \phi_L & \cdots & \phi_1 & 1 \end{bmatrix}^{-1} \begin{bmatrix} 1 \\ 0 \\ \vdots \\ \vdots \\ \vdots \\ 0 \end{bmatrix}. \tag{18}$$

Step 2 $f_m^*, f_{m+1}^*, \cdots, f_{m+l-1}^*$ are determined by $\phi_R(\lambda)$ and the l-simple zeros, $\lambda_1, \lambda_2, \cdots, \lambda_l$, of $N(\lambda)$:

$$\begin{bmatrix} f_m^* \\ f_{m+1}^* \\ \vdots \\ f_{m+l-1}^* \end{bmatrix} = \begin{bmatrix} 1 & \lambda_1 & \cdots & \lambda_1^{l-1} \\ 1 & \lambda_2 & \cdots & \lambda_2^{l-1} \\ \vdots & \vdots & \vdots & \vdots \\ 1 & \lambda_l & \cdots & \lambda_l^{l-1} \end{bmatrix}^{-1} \begin{bmatrix} g(\lambda_1) \\ g(\lambda_2) \\ \vdots \\ g(\lambda_l) \end{bmatrix}, \tag{19}$$

where

$$g(\lambda) := \frac{1}{\lambda^m \phi_R(\lambda)} - \sum_{i=0}^{m-1} f_i^* \lambda^{i-m}.$$

Based on the above results, the preview feedforward controller can be parameterized by

$$\bar{K}_1(\lambda)=\bar{K}_1^*(\lambda)+\phi_R(\lambda)\tilde{K}_1(\lambda), \quad \tilde{K}_1(\lambda)\in\mathbf{R}[\lambda]\cup\mathbf{R}[z], \tag{20}$$

where $\bar{K}_1^*(\lambda)$ is the minimum settling-time deadbeat controller and $\tilde{K}_1(\lambda)$ is any polynomial in λ and z.

To design a $\tilde{K}_1(\lambda)\in\mathbf{R}[\lambda]\cup\mathbf{R}[z]$ that optimizes the transient response, first, choose two appropriate positive integers, p (the parameter related to the settling-time) and q (the number of preview steps), and a non-zero polynomial

$$\begin{aligned}\tilde{K}_1(\lambda)&=\tilde{k}_{-p}\lambda^p+\cdots+\tilde{k}_{-1}\lambda+\tilde{k}_0+\tilde{k}_1 z+\cdots+\tilde{k}_q z^q\\&=z^q(\tilde{k}_{-p}\lambda^{p+q}+\cdots+\tilde{k}_0\lambda^q+\cdots+\tilde{k}_q):=z^q\hat{K}_1(\lambda),\end{aligned} \tag{21}$$

and let $n_{K1}=p+q$, $L_\theta=L+l+n_{K1}$ and $L_\xi=L+n+n_{K1}$. Then,

$$\begin{aligned}e(\lambda)&=[1-N(\lambda)\bar{K}_1(\lambda)]\frac{\bar{r}(\lambda)}{\phi_R(\lambda)}\\&=z^{q-m}\left[\lambda^{q-m}f^*(\lambda)\bar{r}(\lambda)-b(\lambda)\bar{r}(\lambda)\hat{K}_1(\lambda)\right]:=z^{q-m}\sum_{i=0}^{L_\theta-1}\bar{e}_i\lambda^i;\end{aligned} \tag{22}$$

$$\begin{aligned}u_W(\lambda)&=G_{u_W r}(\lambda)r(\lambda)=D(\lambda)\bar{K}_1(\lambda)\frac{\bar{r}(\lambda)}{\phi_R(\lambda)}\\&=\frac{D(\lambda)\bar{r}(\lambda)\bar{K}_1^*(\lambda)}{\phi_R(\lambda)}+z^qD(\lambda)\bar{r}(\lambda)\hat{K}_1(\lambda)\end{aligned} \tag{23}$$

are obtained from Eqs. (2), (14), (15) and (20). Decomposing the first term in the last equation of Eq. (23) yields

$$\begin{cases}\dfrac{D(\lambda)\bar{r}(\lambda)\bar{K}_1^*(\lambda)}{\phi_R(\lambda)}=\dfrac{\beta(\lambda)}{\phi_R(\lambda)}+\alpha(\lambda),\\ \beta(\lambda)=\beta_0+\beta_1\lambda+\cdots+\beta_{L-1}\lambda^{L-1},\\ \alpha(\lambda)=\alpha_0+\alpha_1\lambda+\cdots+\alpha_{L+n-2}\lambda^{L+n-2}.\end{cases} \tag{24}$$

So, the transient part of the weighted control input is

$$\begin{aligned}\Delta u_W(\lambda)&=z^q\left[\lambda^q\alpha(\lambda)+D(\lambda)\bar{r}(\lambda)\hat{K}_1(\lambda)\right]\\&:=z^q\sum_{i=0}^{L_\xi-1}\Delta\bar{u}_{Wi}\lambda^i.\end{aligned} \tag{25}$$

The performance index describing the transient response is defined to be

$$J=\sum_{i=0}^{L_\theta-1}\bar{e}_i^2+\rho^2\sum_{i=0}^{L_\xi-1}\Delta\bar{u}_{Wi}^2. \tag{26}$$

If we define

$$\begin{cases}\bar{e}^*(\lambda):=\displaystyle\sum_{i=0}^{L_\theta-p-2}\bar{e}_i^*\lambda^i=\lambda^{q-m}f^*(\lambda)\bar{r}(\lambda),\\ \Delta\bar{u}_W^*(\lambda):=\displaystyle\sum_{i=0}^{L_\xi-p-2}\Delta\bar{u}_{Wi}^*\lambda^i=\lambda^q\alpha(\lambda),\\ \theta(\lambda):=\displaystyle\sum_{i=0}^{L+l-1}\theta_i\lambda^i=b(\lambda)\bar{r}(\lambda),\\ \xi(\lambda):=\displaystyle\sum_{i=0}^{L+n-1}\xi_i\lambda^i=D(\lambda)\bar{r}(\lambda),\end{cases} \tag{27}$$

then, according to the $\mathcal{H}_2$ optimization method, the $\tilde{K}_1$ in (21) that minimizes J is given by the following theorem.

THEOREM 2 *The coefficient vector of $\tilde{K}_1(\lambda) \in \mathbf{R}[\lambda] \cup \mathbf{R}[z]$ that minimizes the performance index J in (26) is*

$$[\,\tilde{k}_q \quad \cdots \quad \tilde{k}_0 \quad \tilde{k}_{-1} \quad \cdots \quad \tilde{k}_{-p}\,]^T = F_1^{-1} F_2, \tag{28}$$

where

$$F_1 = \begin{bmatrix} \Theta^T & -\rho\Xi^T \end{bmatrix} \begin{bmatrix} \Theta \\ -\rho\Xi \end{bmatrix}, \tag{29}$$

$$F_2 = \begin{bmatrix} \Theta^T & -\rho\Xi^T \end{bmatrix} \begin{bmatrix} E^* \\ -\rho\Delta U_W^* \end{bmatrix}, \tag{30}$$

$$\Theta = \begin{bmatrix} \theta_0 & & \mathbf{0} \\ \vdots & \ddots & \\ \theta_{L+l-1} & \ddots & \theta_0 \\ & \ddots & \vdots \\ \mathbf{0} & & \theta_{L+l-1} \end{bmatrix} \in \mathbf{R}^{L_\theta \times (n_{K1}+1)}, \tag{31}$$

$$\Xi = \begin{bmatrix} \xi_0 & & \mathbf{0} \\ \vdots & \ddots & \\ \xi_{L+n-1} & \ddots & \xi_0 \\ & \ddots & \vdots \\ \mathbf{0} & & \xi_{L+n-1} \end{bmatrix} \in \mathbf{R}^{L_\xi \times (n_{K1}+1)}, \tag{32}$$

$$E^* = [\,\bar{e}_0^* \quad \bar{e}_1^* \quad \cdots \quad \bar{e}_{L_\theta-p-2}^* \quad \mathbf{0}_{p+1}\,]^T, \tag{33}$$

$$\Delta U_W^* = [\,\Delta\bar{u}_{W0}^* \quad \cdots \quad \Delta\bar{u}_{W(L_\xi-p-2)}^* \quad \mathbf{0}_{p+1}\,]^T \tag{34}$$

with elements of the matrices and vectors of Eqs. (31) - (34) being given by Eq. (27). The minimum of J is

$$J_{\min} = J_M - F_2^T F_1^{-1} F_2, \quad J_M = \|E^*\|_2^2 + \rho^2 \|\Delta U_W^*\|_2^2 \,. \tag{35}$$

5 Simulation and Experimental Results

We applied the design method explained in Sections 3 and 4 to the positioning control of an arm robot (Fig. 3) and employed a proportional-positioning minor control loop in the plant to make control easy. The mathematical model of the plant is

$$\begin{cases} \dot{x}_P(t) = \begin{bmatrix} 0 & 1 \\ -\beta & -\alpha \end{bmatrix} x_P(t) + \begin{bmatrix} 0 \\ \beta \end{bmatrix} u_P(t), \\ y(t) = [\,1 \quad 0\,]\, x_P(t), \end{cases} \tag{36}$$

where $y(t)$, $x_P(t) := [\,y(t) \quad \dot{y}(t)\,]^T$ and $u_P(t)$ are the position of the arm, the state of the plant and the voltage command, respectively. Variations in the inertial load etc. are reflected in parameters α and β. Without an additional inertial load, $\alpha_M = 8.33$ and $\beta_M = 69.4$. Brass rods were used to simulate different loads. For the heaviest load (diameter: 15 mm; length: 10 mm), $\alpha_m = 4.17$ and $\beta_m = 34.7$. So, α and β can take the following values $\alpha \in [\alpha_m, \alpha_M]$

and $\beta \in [\beta_m, \beta_M]$. Let

$$\begin{cases} \bar{\alpha} = (\alpha_M + \alpha_m)/2; & \delta_\alpha = (\alpha_M - \alpha_m)/2, \\ \bar{\beta} = (\beta_M + \beta_m)/2; & \delta_\beta = (\beta_M - \beta_m)/2, \\ A_P = \begin{bmatrix} 0 & 1 \\ -\bar{\beta} & -\bar{\alpha} \end{bmatrix}; & B_P = \begin{bmatrix} 0 \\ \bar{\beta} \end{bmatrix}; \quad C_P = [1 \quad 0], \\ \Phi = \begin{bmatrix} 0 & 0 \\ 1 & 1 \end{bmatrix}; & \Gamma(t) = \begin{bmatrix} \frac{\beta - \bar{\beta}}{\delta_\beta} & 0 \\ 0 & \frac{\alpha - \bar{\alpha}}{\delta_\alpha} \end{bmatrix}, \\ \Psi_A = \begin{bmatrix} -\delta_\beta & 0 \\ 0 & -\delta_\alpha \end{bmatrix}; & \Psi_B = \begin{bmatrix} \delta_\beta \\ 0 \end{bmatrix}. \end{cases}$$

Then, the plant (36) can be expressed in the form of Eq. (1). The nominal plant is $\bar{\alpha} = 6.25$ and $\bar{\beta} = 52.1$.

We designed TDF tracking controllers that robustly stabilize the control system for which the output tracks the reference input

$$r(t) = \sin\frac{2\pi}{2.41}t + \sin\frac{4\pi}{2.41}t$$

without steady-state error at the sampling points. For a sampling period of $\tau = 0.01$ s, the internal model of the reference input is given by

$$\phi_R(\lambda) = 1 - 3.9966\lambda + 5.9932\lambda^2 - 3.9966\lambda^3 + \lambda^4. \tag{37}$$

A feedback controller was designed for $Q_u = 1, Q_P = \mathrm{diag}\{1, 0\}, Q_R = I_4$. Theorem 1 yields an output feedback controller with an order of *one* ($n_P - 1 = 1$). The resulting feedback controller $K_2(\lambda)$ is

$$K_2(\lambda) = \left[\begin{array}{c|c} A_{K2} & B_{K2} \\ \hline C_{K2} & D_{K2} \end{array}\right],$$

$$A_{K2} = -0.7548; \quad C_{K2} = 81.48,$$

$$B_{K2} = [9.065 \quad 0.3251 \quad -1.064 \quad 1.171 \quad -0.4335],$$

$$D_{K2} = [-613.5 \quad -84.33 \quad 275.7 \quad -302.8 \quad 112.0],$$

and the controller $K_{2P}(\lambda)$ is

$$K_{2P}(\lambda) = \left[\begin{array}{c|c} -0.7548 & 9.065 \\ \hline 81.48 & -613.5 \end{array}\right].$$

A feedforward controller was designed for the nominal plant with the local feedback controller

$$G(\lambda) = \frac{0.01\lambda\left(2.009\lambda^2 + 4.713\lambda + 2.717\right)}{\lambda^3 + 2.730\lambda^2 + 2.806\lambda + 11.74}$$

for $\rho = 1$ (Eq. (26)). The weighting function $W_u(\lambda) = D_G(\lambda)/D_P(\lambda)$ was selected because it produced the smallest tracking error and control input in our trials.

The performance index for the feedforward controller with the minimum settling-time is $J_M = 3929$. Since $J_{\min}$ decreases monotonically with respect to p and q, and calculations show that, to minimize the performance index, increasing q is much more efficient than increasing p, first, we chose $p = 4$ and $q = 0$ to design a feedforward controller without preview. The performance index was $J_{\min} = 949.5$. Next, we chose $p = 4$ and $q = 4$ to design a preview feedforward controller. The performance index was reduced to $J_{\min} = 7.201$, which is much smaller than the index without preview. The resulting feedforward controller is given by

$$K_1(\lambda) = \frac{N_{K1}(\lambda)}{1+0.7548\lambda},$$
$$N_{K1}(\lambda) = 12.82z^4 - 15.57z^3 - 4.591z^2 + 301.0z$$
$$-27.68 - 64.54\lambda - 4.726\lambda^2 + 18.18\lambda^3 + 1.468\lambda^4$$
$$-6.142\lambda^5 - 1.791\lambda^6 + 12.03\lambda^7 - 6.343\lambda^8.$$

The simulation results (Fig. 5) show that, for the nominal plant, the tracking error is very low when the reference is input, and the applied voltage during the transient response is moderately restricted. For the heaviest inertial load, the system still remains stable and its output tracks the reference input without steady-state error.

The experimental system is shown in Fig. 4. Figure 6 shows the results for the heaviest load. Just as for the simulation results, the control system is stable even when the load is changed; and during the transient response, the tracking error is very low. On the other hand, since the experimental system was originally designed for student practice, the precision is not very high (optical encoder: 16 cycles per turn; gear box: 64.8:1). The voltage applied to the motor reached saturation (± 5 V), and the influence of the dead zone was marked. For these reasons, the response was not as good as the simulations; but the features of the design method, namely, the robust stability resulting from the sampled-data $\mathcal{H}_\infty$ control and the quick response due to the preview were demonstrated by the experimental results.

6 Conclusions

This paper describes a design method for digital tracking control systems for a continuous plant with structured uncertainties. A TDF tracking control system configuration is employed. Regarding the feedback controller, in order to robustly stabilize a plant with structured uncertainties, the design problem is first formulated as a sampled-data $\mathcal{H}_\infty$ control problem, and then transformed into an equivalent discrete-time $\mathcal{H}_\infty$ control problem. A reduced-order output feedback controller with an order less than that of the plant has been designed. The feedforward controller is parameterized based on the feedback controller, with the free parameter being chosen to achieve the desired transient response using a preview strategy. The design method was applied to the control of an arm robot, and the results of both simulations and experiments demonstrate that the integration of a TDF control system configuration, sampled-data $\mathcal{H}_\infty$ control and preview control is a powerful tool for the control of mechatronic systems.

References

[1] Vidyasagar, M., 1985, *Control System Synthesis: A Factorization Approach*, The MIT Press.

[2] Hara, S. and Sugie, T., 1988, "Independent Parameterization of Two-Degree-of-Freedom Compensators in General Robust Tracking Systems," *IEEE Trans. Automat. Contr.*, Vol. 33, pp. 59-67.

[3] Bamieh, B. A. and Pearson, J. B., 1992, "A general framework for linear periodic systems with applications to $\mathcal{H}_\infty$ sampled-data control," *IEEE Trans. Automat. Contr.*, Vol. 37, pp. 418-435.

[4] Kabamba, P. T. and Hara, S., 1993, "Worst-case analysis and design of sampled-data control systems," *IEEE Trans. Automat. Contr.*, Vol. 38, pp. 1337-1357.

[5] Jayasuriya, S. and Tomizuka, M., 1992, "Generalized Feedforward Controllers, Perfect Tracking and Zero Phase Error," *Japan/USA Symposium on Flexible Automation*, Vol. 1, pp. 511-514.

[6] Tomizuka, M., 1993, "On the design of digital tracking controllers," *Trans. ASME, J. Dynam. Sys., Measu., Contr.*, Vol. 115, pp. 412-418.

[7] Tsao, T.-C., 1994, "Optimal Feed-Forward Digital Tracking Controller Design," *Trans. ASME, J. Dynam. Sys., Measu., Contr.*, Vol. 116, pp. 583-692.

[8] Xin, X., Guo, L. and Feng, C., 1996, "Reduced-order controllers for continuous and discrete-time singular $\mathcal{H}_\infty$ control problems based on LMI," *Automatica*, Vol. 32, pp. 1581-1585.

[9] Ohyama, Y., She, J.-H. and Watanabe, K., 1999, "A Prototype Internet Experiment System for Control Engineering," *1999 IEEE Int. Conf. on Systems, Man, and Cybernetics*, Vol. 1, pp. 894-898.

[10] Sivashankar, N. and Khargonekar, P. P., 1993, "Robust stability and performance analysis of sampled-data systems," *IEEE Trans. Automat. Contr.*, Vol. 38, pp. 58-69.

[11] Gahinet, P. and Apkarian, P., 1994, "A linear matrix inequality approach to $\mathcal{H}_\infty$ control," *Int. J Robust & Nonlinear Control*, Vol. 4, pp. 421-448.

Captions of Figures

Figure 1. Configuration of two-degree-of-freedom robust tracking control system.

Figure 2. Design of feedback controller.

Figure 3. Arm robot.

Figure 4. Photograph of the experimental system.

Figure 5. Simulation results of optimal preview response for the nominal plant (solid) and the heaviest inertial load (dotted).

Figure 6. Optimal preview response for the heaviest inertial load (experiment).

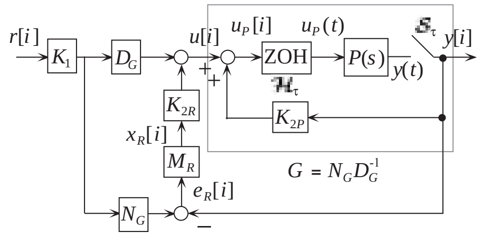

Figure 1: Configuration of two-degree-of-freedom robust tracking control system.

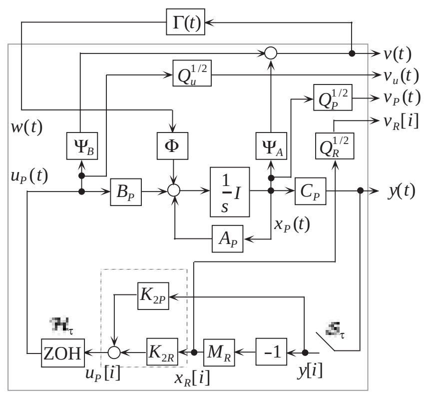

Figure 2: Design of feedback controller.

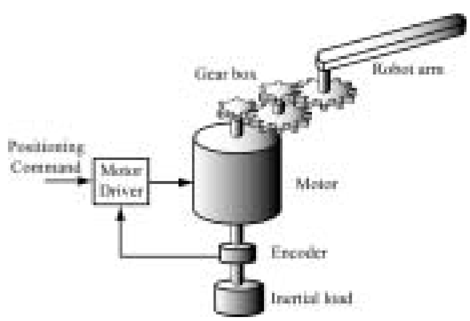

Figure 3: Arm robot.

Figure 4: Photograph of the experimental system.

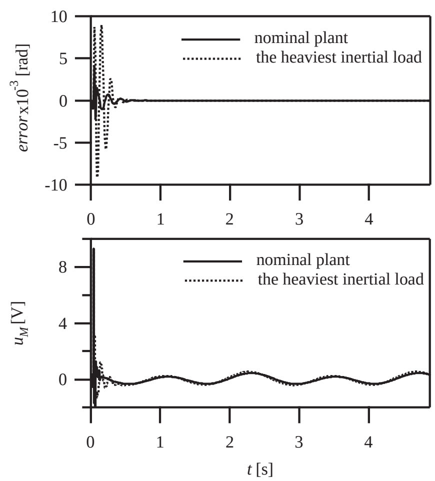

Figure 5: imulation results of optimal preview response for the nominal plant (solid) and the heaviest inertial load (dotted).

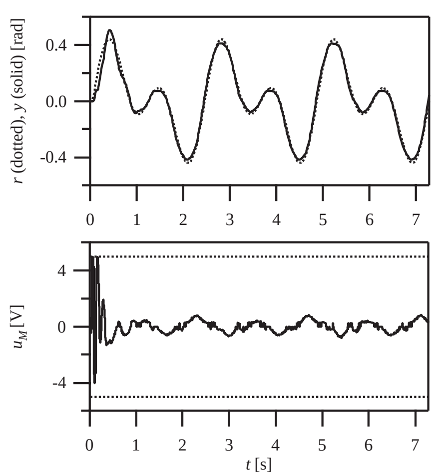

Figure 6: Optimal preview response for the heaviest inertial load (experiment).